Model-Based Evaluation of Methods for Maximizing Efficiency and Effectiveness of Hydraulic Fracture Stimulation of Horizontal Wells

C. Cheng[1], A. P. Bunger[2,1,*]

[1]*Department of Chemical and Petroleum Engineering, University of Pittsburgh, Pittsburgh, PA, USA*

[2]*Department of Civil and Environmental Engineering, University of Pittsburgh, Pittsburgh, PA, USA*

[*]*Corresponding Author:* bunger@pitt.edu

Key Points

- Evaluating options for promoting uniform hydraulic fracture growth and maximizing fracture area.
- High pressure "large limited entry" can be effective when most stress variation is from in-situ stress instead of fracture interaction.
- A lower pressure option with non-uniform fracture spacing is most effective when stress variation is mainly due to fracture interaction.

Abstract

Hydraulic fracturing enables oil and gas extraction from low-permeability reservoirs, but there remains a need to reduce the environmental footprint. Resource use, contaminant-bearing flowback water, and potential for induced seismicity are all scaled by the volume of injected fluid. Furthermore, the greenhouse gas emissions associated with each extracted unit of energy can be decreased by improving resource recovery. To minimize fluid use while maximizing recovery, a rapidly-computing model is developed and validated to enable the thousands of simulations needed to identify opportunities for optimization. Lower pumping pressure approaches that minimize pressure loss through the wellbore perforations combined with non-uniform spacing are shown to be capable of substantially reducing fluid consumption and/or increasing created fracture surface area when the stress variation is mainly from fracture interaction instead of in-situ stress. When in-situ stress variation is dominant, "limited entry" methods promote more uniform growth but with higher pumping pressures and energy consumption.

Plain Language Summary

This paper identifies opportunities to drastically reduce (predicted for some cases up to 65%) water use associated with hydraulic fracture stimulation of low permeability (i.e. shale) oil/gas reservoirs with minimal impact on recovery rates. It also identifies opportunities to increase (up to 120%) the recovery rates of oil/gas for the same injected volume (i.e. keeping the injected volume the same). The key lies in leveraging the mechanics of fracture interaction to produce arrays of hydraulic fractures that are as uniform as possible while balancing an intrinsic trade-off between fracture aperture and surface area. To achieve optimal outcomes, there are different strategies including promoting uniform fracture growth by designing treatments with large pressure loss as fluid flow through the perforations in the casing and into the fracture (so-called "limited entry" method) and selecting non-uniform fracture spacing that balances the stresses induced by fracture growth. Through thousands of simulations enabled by a rapidly-computing simulator, we find different strategies are advantageous depending upon the reservoir conditions and most notably on the variability and/or uncertainty in the in-situ stress. This work therefore highlights an area of ongoing research capable of having an enormous, global impact on the environmental footprint of shale gas/oil production.

1. Introduction

Hydraulic fracturing (HF) is a well-stimulation technique used in oil and gas wells for nearly 70 years. One modern manifestation of this method, multistage fracturing of horizontal wells, uses 8-40 million liters (2-10 million gallons) of water to fracture a single well (Kargbo et al., 2010). Concern has been raised over the increasing quantities of water for hydraulic fracturing in areas that experience water stress, particularly in arid or semi-arid regions, such as China's Ordos Basin (Smakhtin et al., 2004; EIA, 2011) and the United States' Eagle Ford formation and the Permian Basin (Scanlon et al., 2014; Kondash et al., 2018). In some areas, for example the Marcellus shale play in the Appalachian Basin, water is relatively plentiful but transportation is difficult and disposal options for flowback water are limited (Brantley et al., 2018; Mitchell et al., 2013).

The particularities of water-related problems can therefore be specific to a region. However, the overall commonality is that water management presents one of the greatest challenges to both the present and future development of onshore oil and gas development throughout the world. Water-related challenges and impacts can include resource scarcity (e.g., Smakhtin et al., 2004; Scanlon et al., 2014; Kondash et al., 2018), flowback of contaminated water (e.g., Shrestha et al., 2017; He et al., 2017; Sun et al., 2013; Xiong et al., 2016), pollution associated resource transportation (e.g., Brantley et al., 2018; Mitchell et al., 2013; Vengosh et al., 2014; Entrekin et al., 2018), and injection-induced seismicity (e.g., Ellsworth, 2013; Fischer, 2011; Guglielmi et al., 2015). These, and indeed most water-related challenges, risks, and impacts essentially scale in magnitude with the volume of fluid used for hydraulic fracturing (Vengosh et al., 2014; Entrekin et al., 2018; Ellsworth, 2013). Thus motivated, here we focus on two ways the process of extracting oil and/or gas from shale can move towards lower intensity of resource use per resource recovered. The first is reducing resource consumption associated with hydraulic fracturing processes. Additionally, because there is not only a monetary, but also an environmental and societal cost to every well, it is arguably of equal importance to maximize return on the investment by ensuring the best-possible recovery rates. Indeed, among other things, the greenhouse gas (GHG) emissions per unit of energy produced (i.e. kg CO_2eq/MWh) associated with drilling and completion of wells is inversely proportional to the so-called "estimated ultimate recovery" (EUR). (Laurenzi & Jersey, 2013; Vafi & Brandt, 2016) Hence, high resource usage efficiency will reduce GHG emissions, and so this paper will also address a second objective, which is to explore opportunities to increase resource recovery rates.

An important opportunity for reduction of injected volume and/or increasing of recovery rates lies in the widespread observation that 20 to 40 percent of perforation clusters do not contribute significantly to production (Miller et al., 2011). Horizontal wells are stimulated by injection through clusters of holes ("perforations") in the casing that connect the well to the surrounding formation. Typically, stimulation takes places in stages, with the intention for 3-6 of these perforation clusters to be stimulated simultaneously as a part of a single stage. One driving factor for the non-uniformity of production from these perforation clusters is the non-uniformity of in-situ stresses, along the well (e.g., Baihly et al., 2010; Cipolla et al., 2011). "Stress shadowing" is another factor, referring to the suppression of some HFs as a result of the compressive stresses exerted on them by nearby HFs (e.g., Sesetty & Ghassemi, 2013; Abass et al., 2009; Fisher et al., 2004; Meyer & Bazan, 2011), illustrated by the sketch in Figure 1b. Such uneven growth will drive a non-uniform fluid distribution, which inefficiently utilizes the injection fluid (and indeed the wellbore that has been drilled), thus decreasing the efficiency of resource usage.

Here we compare and contrast two approaches to mitigating non-uniform fracture growth. The first has become common practice and entails designing the well perforations so that the pressure drop associated with flow through these holes in the casing is similar to or greater than the pressure associated with hydraulic fracture growth (Howard & Fast, 1970; Weng et al. 1993; Lecampion & Desroches, 2015). This so-called “limited entry” (or “extreme limited entry” when the perforation pressure drop is several times greater than the fracturing pressure) promotes uniform fluid distribution by using the perforation holes like hydraulic chokes. However, as with any mechanism that increases near wellbore friction loss, it comes with a cost of raising overall pumping pressure and hence the pumping power requirements, costs, and CO_2 emissions are increased. Another approach that is predicted by models (Peirce & Bunger, 2015), but remains relatively untested in the field is to manipulate other variables in order to mitigate the tendency of stresses generated by growing fractures to lead to suppression of some fractures and dominance of other fractures (so-called “stress shadow”). By using a rapidly-computing simulator that gives sufficiently accurate approximation to high fidelity models (C5Frac), it is practical to run the thousands of evaluations needed to reveal the conditions under which each strategy is expected to be advantageous.

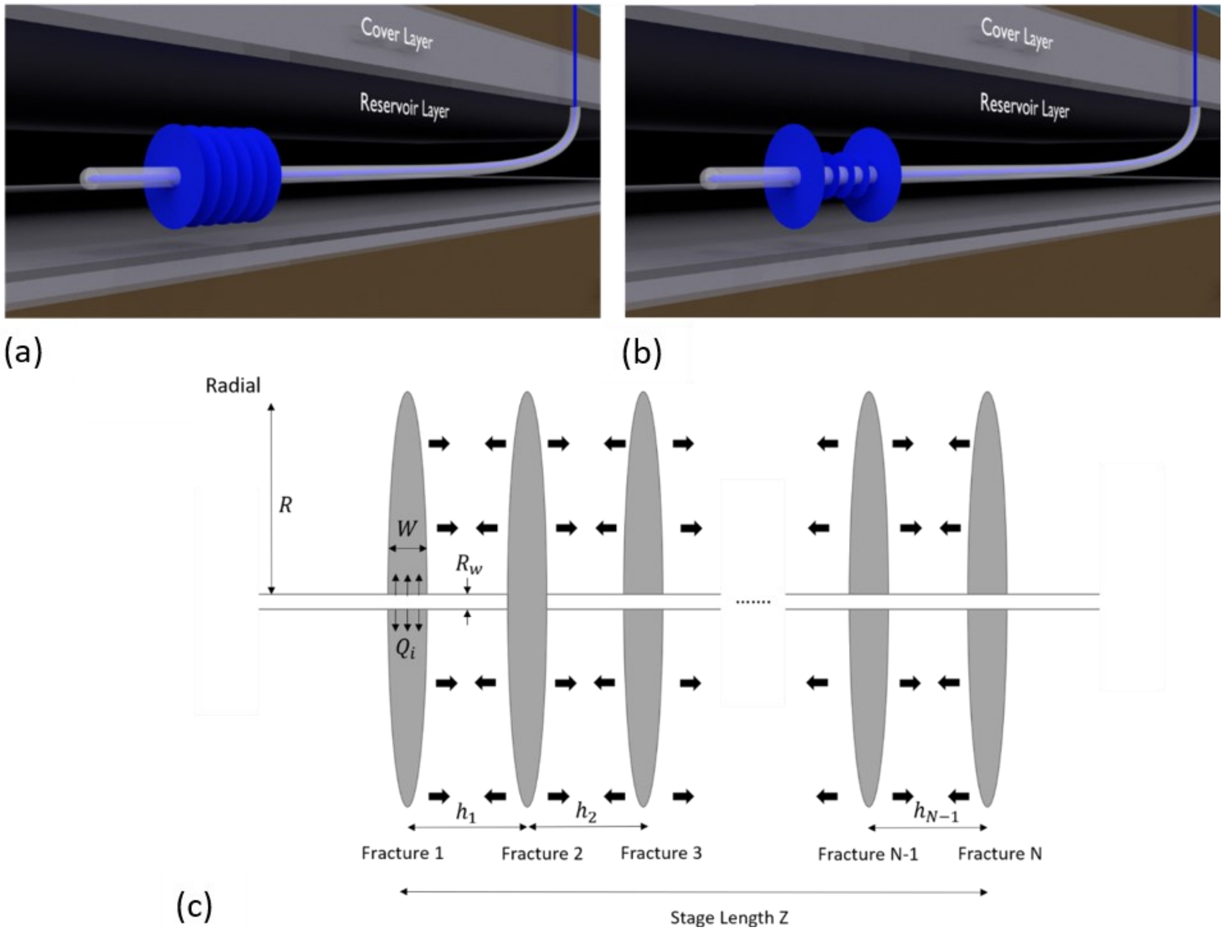

Figure 1. Illustration of multiple, simultaneous HFs in one stage. (**a**) Ideal, uniform result, and (**b**) Result in which central fractures are suppressed. (**c**) Geometry of the multiple HF problem for *N* HFs distributed within a stage of length *Z* and with fracture spacing h_k. The arrows illustrate the interaction stresses between fractures. Figure adapted from (Cheng & Bunger, 2016).

2. Methods

To leverage the opportunity for optimization provided by non-uniform stimulation of perforation clusters, a model is required. But optimizing is challenging due to a variety of well-documented difficulties (Abass et al., 2009) that combine to make high-fidelity simulation time-consuming. Optimization that requires hundreds to thousands of model evaluations is impractical with high-fidelity models.

For this reason, a first step enabling optimizing the resource use and resource recovery is to address the need for rapid, even if approximate, simulation including capturing the transition behavior between multiple fracture growth regimes. We previously demonstrated the feasibility and basic concept of a new HF simulator, C4Frac, which very rapidly simulates the growth of an array of HFs (Cheng & Bunger, 2019). In this prototype reduced order model (ROM), the fractures created from all perforation clusters were restricted to radial, planar growth under the limitation that fractures propagate without toughness (i.e. energy dissipated in fluid flow greatly exceeds energy dissipated due to rock breakage). In the present work, we introduce a modified method to incorporate the toughness into the model so that it is possible to simulate the impact of fluid flow, rock breakage, and fluid loss to the formation ("leak-off") on the growth of multiple, simultaneously-growing hydraulic fractures. In addition to the time-saving provided by the new method, the accuracy is also verified through comparison to benchmark solutions. The model, and its validation, are described in detail in the Supplementary Materials, with a brief overview provided here.

The model considers an array of N simultaneously-growing hydraulic fractures, shown in Figure 1c. For this system, there are $6N$ unknowns which comprise the solution desired from a mechanical model. They are, for each (i^{th}) fracture: 1) the opening (also called "aperture" or "width") $w_i(r,t)$, 2) fluid pressure $p_{f(i)}(r,t)$, 3) fluid flux $q_i(r,t)$, 4) fracture radius $R_i(t)$, 5) elastic interaction stress from the other fractures $\sigma_{I(i)}(r,t)$, and 6) inlet flow rate $Q_i(t)$, where i=1,…,N. The problem consists of solving a system of governing equations in order to find the $6N$ unknown quantities as a function of the given quantities, namely: i) total injection rate Q_O, ii) Carter's leak-off coefficient C_L, iii) viscosity μ, iv) toughness K_{Ic}, v) plane strain elastic modulus E', vi) wellbore radius R_w, vii) spacing (between fracture i and j) $h_{j,i}$, viii) number of fractures

N, and ix) injection time .

2.1. Overall Solution. The solution method and associated assumptions and simplifications follow from our prior work (Cheng & Bunger, 2016; Cheng & Bunger, 2019), but with an important extension that allows for consideration of finite fracture toughness. The prior models were limited to consider cases where energy dissipation associated with rock fracture was negligibly small compared to viscous dissipation associated with fluid flow. The details of the model and its extension are in the Supplementary Materials (SI Section S2). To summarize, the model requires simultaneous solution of $6N$ equations corresponding to the following physical laws:

1) **Volume balance**, where in our ROM we adopt a weak form wherein volume balance is assured globally but not at every location. Additionally, volume balance must account for fluid loss to the formation, and here we follow the widely-used Carter's method to describe the history-dependent leak-off under the assumptions that the hydraulic fracture velocity greatly exceeds the characteristic fluid diffusion velocity in the rock and that the transient fluid net pressure (difference between fluid pressure and in-situ stress in the rock) is much smaller than the difference between the in-situ stress and the undisturbed pore pressure in the reservoir rock (Carter, 1957; Lecampion et al., 2017).
2) **Laminar fluid flow** describing a Newtonian fluid flowing within the fracture according to the classical Poiseuille law. In our ROM we avoid discretization by assuming a functional form that is consistent with known inlet and tip asymptotic behavior, which are the two locations where energy is predominantly dissipated.
3) **Crack propagation** imposing a condition for crack extension according to linear elastic fracture mechanics. In our ROM, we use an approximation whereby the energy dissipated in rock fracture is lumped into a so-called "composite viscosity" such that tip stresses need not

be explicitly computed but energetic equivalence can be maintained via a modification to the resistance to fluid flow.

4) **Elastic crack compliance** providing a relationship between fluid pressure and crack opening satisfying linear momentum balance, strain compatibility, and a linear elastic stress-strain relationship for the rock. In our ROM, the elasticity equation is simplified by restricting growth to the radial geometry, enabling efficient solution for the opening associated with each fluid pressure distribution via a Displacement Discontinuity method (Crouch & Starfield, 1983). Recall that the fluid pressure is taken to follow an assumed functional form that pressure decreases as the fracture volume increase, noting that this behavior contrasts with increasing pressure with volume in the blade-shaped Perkins-Kern-Nordgren (PKN) model. Here we consider just the radial geometry, which captures the most interesting part of the interaction before they reach a high growth barrier provided that the fracture spacing is small enough relative to the barrier height)

5) **Interaction stress** produced in the interior of an elastic solid by the opening of an internal crack, thereby quantifying the stress interaction among the fractures. In our ROM, the interaction stress is computed for each fracture from the analytical solution for a uniformly pressurized crack (Sneddon, 1946) with an equivalent volume.

6) **Inlet pressure continuity and inlet volume balance** enforcing that the pressures at the inlets of each fracture are equal, that is, tied to the same wellbore and assuming negligible fluid pressure loss along the wellbore and considering friction loss using the Crump and Conway (1988) model. Additionally, the inlet condition requires the sum of fluid influx to all fractures equals the total injection rate to the wellbore. Imposing this condition requires accurate calculation of the inlet pressure. We use an approach that updates the wellbore pressure so as

to ensure its consistency with the overall energy balance of the system, thereby describing the inlet pressure via more robust integral quantities.

The corresponding governing equations and the details of the solution algorithm used to rapidly computing simultaneous solution to these coupled equations is described in the Supplementary Materials (SI).

2.2. Validation. To check the accuracy of the developed approximate solution, it is necessary to compare predictions of the approximation to reference solutions. In this study, the validation entails two parts. One is benchmarking with a solution for a single hydraulic fracture, using a solution developed by Dontsov (2016). The model compares within a fraction of a percent for most cases, with an error of at most 7% for a certain domain of the solution where leak-off is small and fracture toughness and fluid viscosity have similar magnitudes of energy dissipation. This favorable benchmark, detailed in SI (Section S4.1), validates the solution method for the hydraulic fracture model. Furthermore, validation for cases with multiple fractures entails comparing to high-fidelity model results ("ILSA II" (Peirce & Bunger, 2015) developed from "ILSA" (Peirce & Detournay, 2008)). This validation is also achieved, and is detailed in the SI (Section S4.2). Strong agreement with the high-fidelity model, especially for the fracture area generated by each configuration, demonstrates that the approach to coupling the interacting fractures leads to an ROM that is useful for the purposes of the optimization considered in the subsequent sections.

3. Results

Before presenting a proof of concept demonstrating use of the approximate simulator for treatment design to pursue higher resource usage efficiency, it is important to adopt a more formal definition of "efficiency of resource usage". The practically-relevant answer relates a measure of estimated ultimate recoveries (EUR) of the well to a measure of the inputs such as materials and associated environmental effect. Because surface area scales to recovery both in classical predictions of production from hydraulic fractures (Economides & Nolte, 2000) and in more recent approaches relating to the Stimulated Reservoir Volume (SRV) (Fisher et al., 2002) (corresponding to the area of hydraulic fractures times the characteristic width of the region of drainage around the hydraulic fractures), here we will adopt the total fracture surface area ($\boldsymbol{A}$) of all the fractures in the array until time t as a proxy for the EUR of well as impacted by an HF treatment. Generating such an output requires inputs, and one of the most direct and measurable inputs is the injection volume. As previously pointed out, a number of environmental impacts and risks scale with the fluid volume, taken as $Q_O t_{TOT}$, where Q_O is the injection rate and t_{TOT} is the total injection time. Hence, an optimally efficient treatment can be considered alternately as one using the least volume of fluid to generate a given fracture area or as one generating the most fracture area for a given volume. Both of these forms of optimality will be examined in the demonstration that follows.

3.1. Minimizing Injection Volume. A smaller injection volume is important to reduce a variety of volume-dependent environmental impacts. Here we will examine the ability to minimize injection volume via optimization that utilizes appropriate viscosity and non-uniform spacing in a complimentary way to produce a desired fracture surface area.

3.1.1. Overall Behavior. Previously we developed reduced order models (ROMs) for estimating growth characteristics of multiple, simultaneously growing hydraulic fractures. These models were limited to the so-called "viscosity dominated" regime, in which the pressure required to overcome energy dissipated by viscous fluid flow within the fracture greatly exceeds the energy associated with rock breakage. While these prior efforts established a basic approach for ROM development for multiple hydraulic fractures, it is useful to extend consideration to all regimes for the purpose of showing the potential for optimization over a larger number of design parameters. In order to demonstrate the dependence of the results upon nominal propagation regime, we adopt the dimensionless quantities after Dontsov (2016).

$$\Phi = \frac{\mu'^3 E'^{11} C_L'^4 Q_o}{K'^{14}}, E' = \frac{E}{(1-\nu 2)}, K' = (\frac{32}{\pi})^{1/2} K_{IC}, \mu' = 12\,\mu \tag{1}$$

$$\tau = \left(\frac{K'^{18} t^2}{E'^{13} \mu'^5 Q_o^3}\right)^{1/2} \tag{2}$$

where E is Young's modulus, ν is Poisson's ratio, K_{IC} is fracture toughness, and μ is dynamic viscosity. With this definition, transition from small to large τ corresponds to a transition from a regime in which viscous dissipation far exceeds rock fracturing to a regime where viscous fluid flow is negligible compare to the fracture propagation. Small Φ corresponds to negligible leak-off, while large Φ corresponds to large leak-off. Hence the lower left corner of Figure 2 corresponds to small leak-off and large viscosity, while the upper right corner corresponds to large leak-off and small viscosity. Note that the cases presented in Figure 2 are in a transition range between the limiting regimes. A more detailed discussion of the limiting and transition regimes is not directly needed in the present illustration of results, but for completeness is included in the SI Section S4.1.

Additionally, it is important to note that the leak-off coefficient C_L is coupled with the fluid viscosity, i.e. higher viscosity leads to lower leak-off. Neglecting any accumulation of particulate/polymer on the fracture comprising a low permeability "filter cake", and further assuming that the fluid injected to the fracture is not too dissimilar in viscosity to the native fluid in the reservoir, the viscosity and leak-off rate are coupled via Carter's leak-off parameter (Carter, 1957; Lecampion et al., 2017).

$$C_L = \sqrt{\frac{k c_r \phi}{\pi \mu}} p_\Delta, p_\Delta = \sigma_o - p_o \tag{3}$$

where k is the rock permeability, c_r is the reservoir compressibility, combining the reservoir fluid and pore compressibility, ϕ is the rock porosity, σ_o is the in-situ stress and p_o is the reservoir pressure. Accordingly, in the parametric studies to follow, Equation 3 is rewritten using $C_{L0} = C_L(\mu = 1\text{Pa.s})$ as the reference leak-off coefficient. Hence for a given fluid viscosity, $C_L = \sqrt{\frac{1\,Pa\,s}{\mu}} C_{L0}$.

As an illustrative example, we show that injection volume can vary significantly depending upon both the nominal regime (location in the plots in Figure 2 as defined by Φ and τ Equations 1 and 2) and the fracture spacing. Specifically we contrast uniformly-spaced and a particular non-uniform spacing, which is inspired from prior work (Cheng & Bunger, 2016; Lecampion et al., 2017; Cheng & Bunger, 2019) demonstrating that some non-uniform spacing configurations can balance the impact of stress shadow acting on the fractures, thereby leading to more uniform fracture growth. This parametric study entails varying viscosity and characteristic leak-off parameter C_{L0}, keeping all other quantities unchanged with practically-relevant values given by

$$\begin{gathered} R_W = 0.2\text{ m}, K_{IC} = 1\text{ MPa}\cdot\text{m}^{\frac{1}{2}}, E = 10\text{ GPa} \\ \nu = 0.2\,, \sigma_o = 70\text{ Mpa}, Q_o = 0.2\text{ m}^3/s, \\ A_{TOT} = 100{,}000\text{ m}^2, \text{Z} = 50\text{ m} \end{gathered} \tag{4}$$

until a fracture surface area of 100,000 m^2 is achieved. Note that the value of area limit is set so as to avoid the total injection time deviating so far from the pumping time required for an average (practical) case, which is usually in the order of tens of minutes (up to, say, 100 minutes at the most). Additionally, we selected non-uniform design with $h_1 = h_4 = 9\text{m}, h_2 = h_3 = 16\text{m}$ and uniform spacing $h_1 = h_2 = h_3 = h_4 = 12.5\text{m}$ as a comparison case with the same injected volume for a total stage length $Z = 50\text{m}$ (recalling definitions in Figure 1). For all cases, the injected volume is computed (Figure 2a and b), and a comparison is then made between uniform and non-uniform cases via the ratio of volume, V_{non}/V_{uni}. To see the effect of varying viscosity, with all other parameters held constant (except the impact of viscosity on C_L accounted for via Equation 3), reference lines for the viscosity and the resulting leak-off coefficient are given in Figure 2.

We can see an advantage is provided by the non-uniform case. We firstly observe that, except for some unpractically high leak-off regions (upper right corner, where the ratio of fracture volume to injected volume is below 5%), the non-uniform spacing always generates more fracture area than uniform spacing. This is especially true when viscosity is near 10^{-1} Pa.s and leak-off is around 10^{-6} $\mathrm{m \cdot s^{1/2}}$; there is a more than 60% decrease in fluid volume in this practically-relevant region. In addition, a decreased volume is achieved in both uniform and non-uniform cases by choosing viscosity in an optimal range.

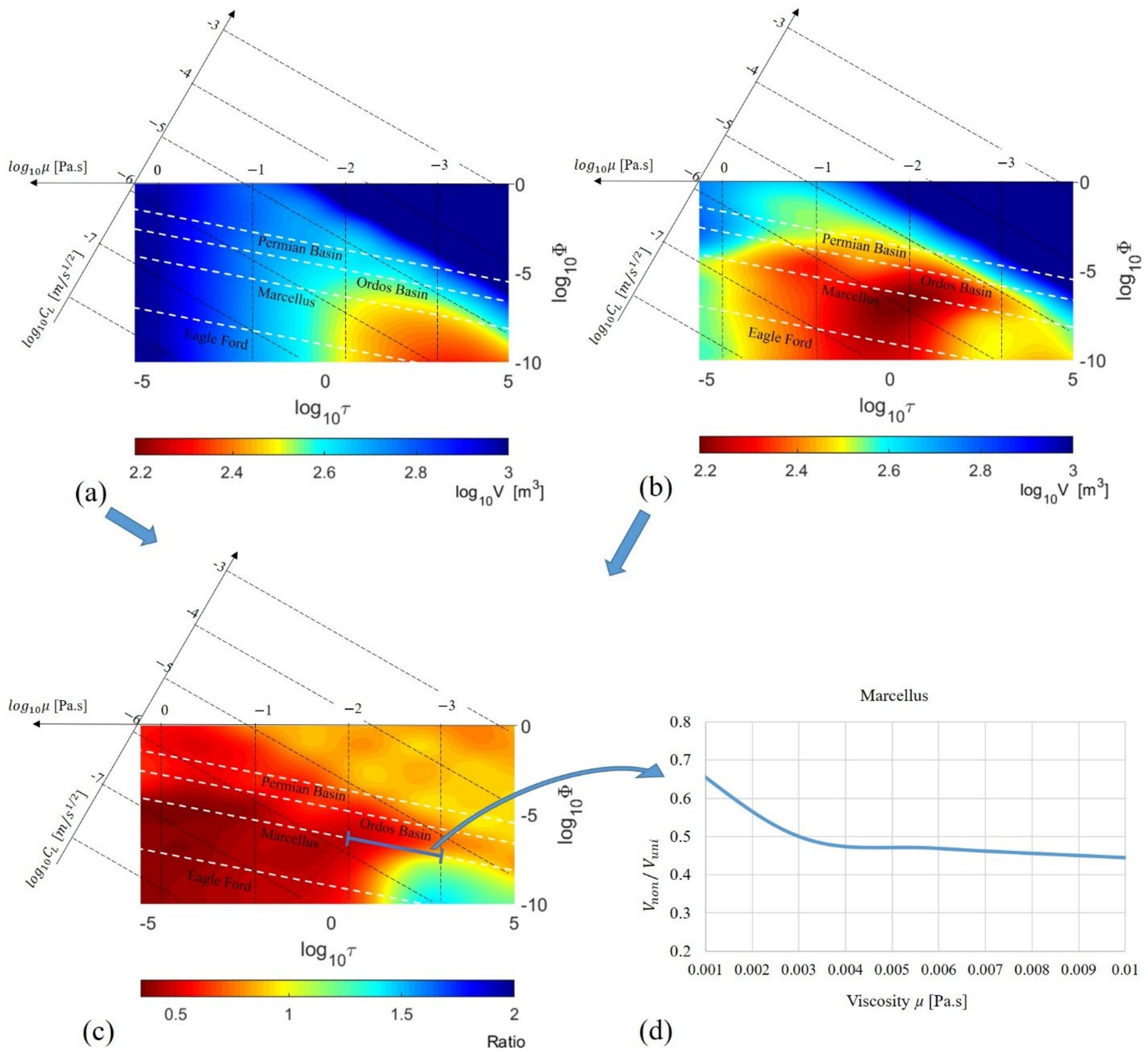

Figure 2. Injection volume in all practical regimes. The injected volume plotted as a function of log (τ) and log (Φ) for non-uniform and uniform space respectively: (**a**) uniform (**b**) non-uniform (**c**) ratio between non-uniform and uniform design. Here contours are shown of varying C_L and μ, with all other parameters according to Equation 4. (d) an example showing a profile of volume versus viscosity along a portion of the dashed line for the Marcellus example.

3.1.2. *Interplay between Limited Entry and Variable In-Situ Stress.* The previous results show that non-uniformity of induced stresses around growing hydraulic fracture arrays leads to suppression of some fractures and favoring of others. In reality, there is also naturally-occurring stress variability due to variation of rock properties along the horizontal wellbore. Hence one can expect that the relative importance of stress shadow versus random stress variation will govern a change in overall behavior of the system and determine the best strategies for promoting uniform fracture growth. As an example, simulations are carried out using rock properties from the Marcellus formation (Table S2). The details of the basin and corresponding parameters are in the Supplementary Materials (SI Section S6). The spacings used here are the same as in Section 3.1.1. Since the most commonly-used fluids are: slick water (0.003Pa.s), linear gel (0.05Pa.s) and crosslinked gel (0.5Pa.s), the graphs are zoomed in on the most instructive range of viscosity 0.003-1Pa.s. To account for the limited entry, the pressure loss though perforation tunnels is embedded into the simulator via the global energy balance using the power expression (Bunger et al., 2014)

$$P_{perf} = aQ_i(t)^3\left(\frac{\rho}{n^2 D_p^4 C^2}\right) \tag{5}$$

The numerical factor, a, is usually taken from Crump and Conway (1988) as 0.8106. The density of injected fluid is ρ. Each cluster has n perforations, D_p represents the perforation diameter, and C is a shape factor for the perforation tunnels. Instead of a specific value for each parameter, here we give a value for the bracketed quantities in Equation 5 to achieve a roughly predicted pressure loss which usually range between 10^4 to 10^7 Pa. As a reference, a common limited entry design in practice involves uniform fracture spacing with $3 * 10^6 - 10^7$ Pa perforation loss. Furthermore, the in-situ stress variation is incorporated into the simulator via its contribution $\dot{W}_{o(i)}$ to the global energy balance

$$\dot{W}_{o(i)} = -\sigma_o(1 \pm S_i)\left(Q_i - 4\pi\frac{C_L R_i^2}{t^{1/2}}\int_0^1 \frac{\rho_i}{\sqrt{\sqrt{1-{\rho_i}^{\alpha_i}}}}d\rho_i\right) \tag{6}$$

where S_i is the variability of the in-situ stress for each stage relative to the average stress σ_o. Details of the derivation are provided in SI Section S2.7. For the simulations, σ_o is set as 30 MPa and the S_i is taken for each case as an array of random values from the range [-v/2,v/2], where v is set at various levels and referred to as the "In-Situ Stress Variation". Latin Hypercube sampling is chosen to ensure that the broadest range of results can be found with the fewest evaluations. Here the number of random S_i between bounds is set as 18, that is, 18 realizations are computed wherein each realization entails randomly drawing S_i, $i=1,\ldots,N$ for each of the N fractures within the stage (N=5 in this example). The maximum and minimum values of all realizations are indicated by the dash dot lines in Figure 3a and b for 2% in-situ stress variation, with the symbols and line giving the average value from all realization. These computed ranges and average values are also portrayed in Figures 3c - f for differing levels of in-situ stress variation, wherein the perforation loss used in optimization is fixed at around 10^5 Pa to compare with the extreme limited entry value of 10^7 Pa. The viscosity corresponding to crosslinked gel is selected in Figure 3c and d for comparison with viscosity of slick water in Figure 3e and f. Results are presented as injected volume required for a given fracture area (namely 100,000 m^2, Figure 3a), fracture area generated by a given injected volume (namely 460 m^3, Figure 3b), and the relative change of these quantities compared to a very large limited entry case which results in essentially uniform fluid distribution among the fractures (Figures 3c-f).

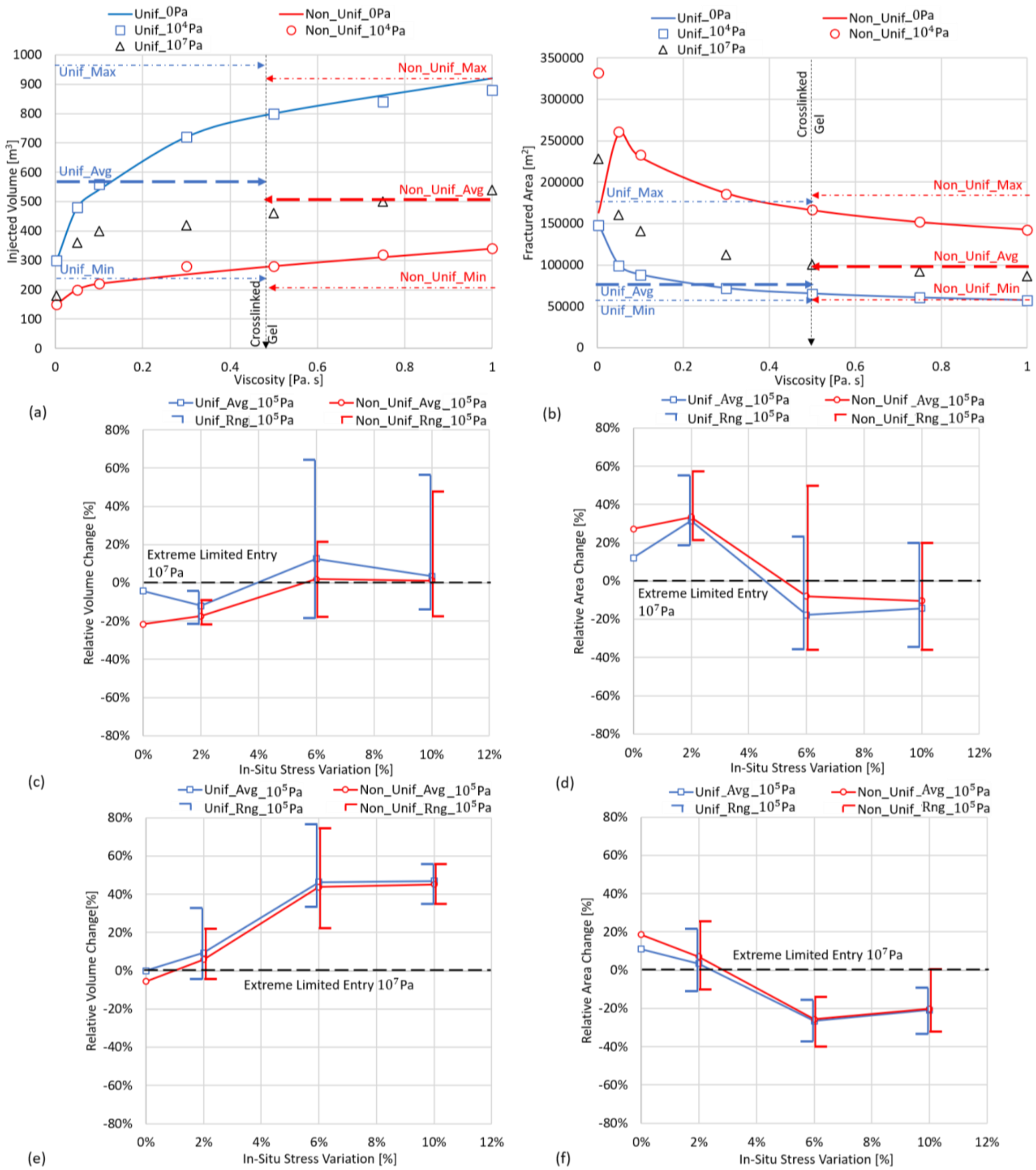

Figure 3. Effect of in-situ stress variation with different fluid viscosities and levels of limited entry. Note that Unif and Non_Unif means uniform and non-uniform spacing, respectively. The last digits indicate the pressure of entry loss. (**a**) Total injected volume comparison for generating 100,000 m^2 of fracture area. (**b**) Total fractured area comparison for injection of 460 m^3 of fluid.

(**c**) For crosslinked gel, the relative volume change of 10^5 Pa compared to 10^7Pa limited entry at different values of in-situ stress variation. (**d**) is for relative fractured area change. (**e**) and (**f**) Relative change in injection volume and fracture area, respectively, for slick water.

The results show that uniform spacing with small limited entry is never the best approach; these cases require more fluid to achieve a given fracture area and produce less fracture area for a given injected volume compared to the other cases. The conclusion is the same for all viscosities and in-situ stress variabilities and can be drawn by viewing average values and/or minimum/maximum values of the ranges.

The results also show that the advantageous choice between large limited entry and non-uniform spacing depends upon the in-situ stress variability. Specifically, if the variability of in-situ stress is below a certain value, in this example about 5%, small limited entry with non-uniform fracture spacing promotes better outcomes than large limited entry. This is to be expected because the advantage of non-uniform spacing requires that the stress shadow generated by the net fluid pressure inside the fractures has to sufficiently exceed the magnitude of the variability of in-situ stress, thereby acting as the dominant stress variability in the system. As Figure 3b shows, 15% less volume consumption and 20% more fractured area is enabled by small limited entry, and the net pressure is around 10^7 Pa, several times greater than the corresponding in-situ stress variability 10^6Pa (at 3%). When the in-situ stress variability is above 6% (2×10^6Pa), which is close to the net pressure (10^7Pa), extreme limited entry performs better. The improved performance is because the pressure increase due to the friction loss dominates the stress variability. This leads to greater uniformity among the simultaneously growing fractures. The shift of advantageous design between small and large limited entry appears as a crossover of average possible outcomes in Figure 3b and c. Note that it is readily confirmed by simulations that large limited entry gives nearly identical results for uniform and non-uniform fractures spacing.

4. Discussion and Conclusions

Resource use efficiency is an issue at the heart of the environmental footprint of hydraulic fracturing. Increasing the resource usage efficiency will lead to less injection per unit recovery and/or more recovery per well leading to relatively lower GHG emissions per unit energy produced. A major challenge to optimization is that many simulation runs are required, thereby motivating development of fast, approximate models. Building on previous versions (Cheng & Bunger, 2019), the new model C5Frac is developed to extend consideration to include the impact of the fracture toughness of the rock and fluid leak-off.

Based on thousands of simulations that are practically enabled by the short computation times required by C5Frac, we first observe that if in-situ stress variation is substantially less than the net pressure associated with driving fracture growth, both large limited entry and non-uniform fracture spacing are effective at promoting uniform distribution of fracture growth. The large limited entry approach leads to higher fluid pressures (hence higher cost and CO_2 emissions from pumping equipment), but gives similar and in some cases lower generated fracture areas compared to small limited entry cases. The main advantage of large limited entry is that the uncertainty in the outcome of the stimulation is much smaller, that is, the range of outcomes collapses to a point. When in-situ stress variability is low, this benefit is less pronounced and arguably not worth the "price". However, if variation of in-situ stress is high, then large limited entry can provide a significant benefit. This benefit is due to the fact that friction loss caused by the perforations provides enough pressure to overwhelm such randomness. Furthermore, in cases with large in-situ stress variation, the balancing of the stress shadow effects provided by non-uniform fracture spacing has a small impact compared to the random stress. Simulation results secondly lead to an overall observation that non-uniform spacing will always equal or improve on uniform spacing counterparts in every sense including error bounds. Specifically, for small limited entry the non-uniform spacing clearly outperforms uniform spacing. This work demonstrates resource use efficiency is optimizable and with optimization depending upon not only deterministic values of reservoir conditions, but also on the variability of those conditions. Hence, these simulations provide impetus for systematic, ongoing, and focused efforts to identify optimizing strategies that account for uncertainty and variability of in situ stress and other rock properties.

Acknowledgments

This material is based upon work supported by the University of Pittsburgh Center for Energy, Swanson School of Engineering, Department of Chemical and Petroleum Engineering, and Department of Civil and Environmental Engineering. Additional support for recent advances to this work was provided by the National Science Foundation under Grant No. 1645246. All data used to generate figures in this paper are made available at http://d-scholarship.pitt.edu/ (searchable by author surnames).

References

Abass, H. H., Soliman, M. Y., Tahini, A. M., Surjaatmadja, J., Meadows, D. L., & Sierra, L. (2009). Oriented fracturing: A new technique to hydraulically fracture an openhole horizontal well. In Proceedings SPE Annual Technical Conference and Exhibition. New Orleans, LA, USA. SPE 124483.

Baihly, J. D., Malpani, R., Edwards, C., Han, SY., Kok, J. C. L., Tollefsen, E. M., & Wheeler, C.W. (2010). Unlocking the shale mystery: How lateral measurements and well placement impact completions and resultant production. In Proceedings SPE Tight Gas Completions Conference. San Antonio, Texas, USA. SPE 138427.

Batchelor, G. K. (1976). Brownian diffusion of particles with hydrodynamic interaction. *Journal of Fluid Mechanics,* 74, 1–29.

Batchelor, G. K. (1967). An Introduction to Fluid Dynamics (Cambridge University Press, Cambridge, UK).

Brantley, S. L., Vidic, R. D., Brasier, K., Yoxtheimer, D., Pollak, J., Wilderman, C., & Wen, T. (2018). Engaging over data on fracking and water quality. Science. 359, 395-397.

Bunger, A. P. (2013). Analysis of the power input needed to propagate multiple HFs. *International Journal of Solids and Structures,* 50, 1538–1549.

Bunger, A. P., Jeffrey, R. G., & Zhang, X. (2014). Constraints on Simultaneous Growth of Hydraulic Fractures from Multiple Perforation Clusters in Horizontal Wells. SPE Journal, 19, 608-620.

Carter, E. (1957). in Optimum fluid characteristics for fracture extension. G. C. Howard, C. R. Fast, Eds. (Drilling and Production Practices), pp. 261–270.

Cheng, C., & Bunger, A. P. (2019). Optimizing Fluid Viscosity for Systems of Multiple Hydraulic Fractures. *AICHE Journal.* DOI:10.1002/aic.16564.

Cheng, C., & Bunger, A. P. (2019). Reduced order model for simultaneous growth of multiple closely-spaced radial hydraulic fractures. *Journal of Computational Physics,* 376, 228-248.

Cheng, C., & Bunger, A. P. (2016). Rapid Simulation of Multiple Radially-Growing HFs Using an Energy-Based Approach. *International Journal for Numerical and Analytical Methods in Geomechanics,* 71, 281–282.

Cheng, C., Bunger, A. P., & Peirce, A. P. (2016). Optimal Perforation Location and Limited Entry Design for Promoting Simultaneous Growth of Multiple Hydraulic Fractures, Society of Petroleum Engineers. doi:10.2118/179158-MS.

Crump, J. B., & Conway, M. W. (1988). Effects of perforation-entry friction on bottomhole treating analysis. Journal of Petroleum Technology, 15474, 1041–1049.

Cipolla, C., Weng, X., Onda, H., Nadaraja, T., Ganguly, U., & Malpani, R. (2011). New algorithms and integrated workflow for tight gas and shale completions. In Proceedings SPE Annual Technology Conference and Exhibition. Denver, Colorado, USA. SPE 146872.

Crouch, S. L., & Starfield, A. M. (1983). Boundary Element Methods in Solid Mechanics (George Allen & Unwin, London).

Desroches, J., Detournay. E., Lenoach, B., Papanastasiou, P., Pearson, J. R. A., Thiercelin, M., & Cheng, A. (1994). The crack tip region in hydraulic fracturing. *Proceedings of the Royal Society of London. Series A,* 447, 39–48.

Detournay, E. (2016). Mechanics of Hydraulic Fractures. *Annual Review of Fluid Mechanics,* 48, 311-339.

Detournay, E., & Peirce, A. (2014). On the moving boundary conditions for a hydraulic fracture. *International Journal of Engineering Science,* 84, 147–155.

Detournay, E. (2004). Propagation regimes of fluid-driven fractures in impermeable rocks. *International Journal of Geomechanics,* 4, 1–11.

Dontsov, E.V. (2016). An approximate solution for a penny shaped hydraulic fracture that accounts for fracture toughness, fluid viscosity and leak-off. *Royal Society Open Science.* 3, 160737

Economides, M., & Nolte, K. G. (2000). Reservoir Stimulation (John Wiley & Sons).

Ellsworth, W. L. (2013). Injection-Induced Earthquakes. *Science.* 341, 142-149.

Energy Information Administration. (2018). Permian Basin Wolfcamp Shale Play Geology review. 2018.

Energy Information Administration. (2017). Marcellus Shale Play Geology review.

Energy Information Administration. (2014). Marcellus Updates to the EIA Eagle Ford Play Maps.

Energy Information Administration. (2012). Annual Energy Outlook 2012.

Energy Information Administration. (2011). World Shale Gas Resources: An Initial Assessment of 14 Regions Outside the United States; EIA, International Energy Statistics; Freedom House, Freedom in the World.

Entrekin, S., Trainor, A., Saiers, J., Patterson, L., Maloney, K., Fargione, J., Kiesecker, J., Baruch-Mordo, S., Konschnik, K., Wiseman, H., Nicot, J. P., & Ryan, J. N. (2018). Water Stress from High-Volume Hydraulic Fracturing Potentially Threatens Aquatic Biodiversity and Ecosystem Services in Arkansas, United States. *Environmental Science & Technology, 52*, 2349-2358.

Fischer, T., & Guest, A. (2011). Shear and tensile earthquakes caused by fluid injection. *Geophysical Research Letters,* 38. L045447.

Fisher, M. K., Heinze, J. R., Harris, C. D., Davidson, B. M., Wright, C. A., & Dunn, K. P. (2004). Optimizing horizontal completion techniques in the Barnett shale using microseismic fracture mapping. In Proceedings SPE Annual Technology Conference and Exhibition. Houston, Texas, USA. SPE 90051.

Fisher, M., Wright, C., Davidson, B., Goodwin, A., Fielder, E., Buckler, W., & Steinsberger, N. (2002). Integrating fracture mapping technologies to optimize stimulations in the Barnett Shale.In SPE Annual Technical Conference and Exhibition. San Antonio, Texas. SPE 77441;

Garagash, D. (2000). Hydraulic fracture propagation in elastic rock with large toughness. in Pacific Rocks 2000 'Rock around the rim', J. Girard, M. Liebman, C. Breeds, T. Doe, Eds (A.A. Balkema, Rotterdam), pp. 221-228.

Guglielmi, Y., Cappa, F., Avouac, J.P., Henry, P., & Elsworth, Derek. (2015). Seismicity triggered by fluid injection–induced aseismic slip, *Science*, 348, 1224-1226.

He,Y., Flynn, S. L., Folkerts, E. J., Zhang, Y., & Goss, Greg. G. (2017). Chemical and toxicological characterizations of hydraulic fracturing flowback and produced water. *Water Research,* 114, 78-87.

Howard, G. C., & Fast, C. R. (1970). Hydraulic fracturing. New York, Society of Petroleum Engineers.

Irwin, G. R. (1957). Analysis of stresses and strains near the end of a crack traversing a plate. *ASME. Journal of Applied Mechanics,* 24, 361–364.

Kanninen, M. F., & Popelar, C. H. (1985). Advanced Fracture Mechanics, in Oxford Engineering Science Series, (Oxford Univ. Press, Oxford, UK), vol. 15.

Kargbo, D. M., Wilhelm, R. G., & Campbell, D. J. (**2010)**. Natural Gas Plays in the Marcellus Shale: Challenges and Potential Opportunities. *Environmental Science & Technology,* 44, 5679-5684.

Kondash, A. J., Lauer, N. E., & Vengosh, A. (2018). The intensification of the water footprint of hydraulic fracturing. *Science Advances,* 4, 5982-5990.

Laurenzi, I. J., & Jersey, G. R. (2013). Life Cycle Greenhouse Gas Emissions and Freshwater Consumption of Marcellus Shale Gas. *Environmental Science & Technology,* 47, 4896-4903.

Lecampion, B., Bunger, A. P., & Zhang, X. (2017). Numerical methods for hydraulic fracture propagation: A review of recent trends. *Journal of Natural Gas Science and Engineering,* 49, 66-83.

Lecampion, B., & Desroches, J. (2015). Simultaneous initiation and growth of multiple radial hydraulic fractures from a horizontal wellbore. Journal of the Mechanics and Physics of Solids, 82, 235–258.

Lecampion, B., & Detournay, E. (2007). An implicit algorithm for the propagation of a hydraulic fracture with a fluid lag. *Computer Methods in Applied Mechanics and Engineering,* 196, 4863-4880.

Meyer, B., & Bazan, L. (2011). A discrete fracture network model for hydraulically induced fractures-theory, parametric and case studies. In Proceedigs SPE Hydraulic Fracturing Technology Conference and Exhibition. The Woodlands, Texas, USA. SPE 140514.6.

Miller, C., Waters, G., & Rylander, E. (2011). Evaluation of production log data from horizontal wells drilled in organic shales. In SPE North American Unconventional Gas Conference and Exhibition, The Woodlands, Tx, USA, 14-16 June 2011. SPE 144326.

Mitchell, A. L., Small, M., & Casman, E. A. (2013). Surface water withdrawals for Marcellus Shale gas development: Performance of alternative regulatory approaches in the Upper Ohio River Basin. *Environmental Science & Technology,* 47, 12669−12678.

Montgomery, C. T. (2013). Fracturing Fluids. In A. P. Bunger, J. McLennan, R. G. Jeffrey, (Eds.), Effective and Sustainable Hydraulic Fracturing. Chapter 1. Rijeka, Croatia: Intech.

National Research Council. (2013). Induced seismicity potential in energy technologies. National Academies Press.

Peirce, A. P., & Bunger, A. P. (2015). Interference Fracturing: Non-Uniform Distributions of Perforation Clusters that Promote Simultaneous Growth of Multiple HFs. SPE Journal, 20, 384-395

Peirce, A. P., & Detournay, E. (2008). An implicit level set method for modeling hydraulically driven fractures. *Computer Methods in Applied Mechanics and Engineering,* 197, 2858-2885.

Rice, J. R. (1968). in Fracture: An Advanced Treatise, H. Liebowitz, Ed. (Academic Press, New York), vol. 2, chap. 3. pp. 191-311.

Ruppel, S. (2019). Stratal Architecture and Facies Development in a Middle Wolfcampian Platform Carbonate Reservoir: University Block 9 Field, Andrews County, Texas.

Savitski, A. A., & Detournay, E. (2002). Propagation of a penny-shaped fluid-driven fracture in an impermeable rock: asymptotic solutions. *International Journal of Solids and Structures,* 39, 6311–6337.

Scanlon, B. R., Reedy, R. C., & Nicot, J. P. (2014). Will water scarcity in semiarid regions limit hydraulic fracturing of shale plays? *Environmental Research Letters,* 9, 124011-124025.

Sesetty, V., & Ghassemi, A. (2013). Numerical simulation of sequential and simultaneous hydraulic fracturing. In A. P. Bunger, J. McLennan, R. G. Jeffrey, (Eds.), Effective and Sustainable Hydraulic Fracturing. Chapter 33. Rijeka, Croatia: Intech.

Spence, D.A., & Sharp, P.W. (1985). Self-similar solution for elastohydrodynamic cavity flow. *Proceedings of the Royal Society of London. Series A,* 400, 289–313.

Shrestha, N., Chilkoor, G., Wilder, J., Gadhamshetty, V., & Stone, J. J. (2017). Potential water resource impacts of hydraulic fracturing from unconventional oil production in the Bakken shale. *Water Research,* 108, 1-24.

Smakhtin, V., Revenga, C., & Doll, P. (2004). A pilot global assessment of environmental water requirements and scarcity. *Water International,* 29, 307−317.

Sneddon, I. N. (1951). Fourier Transforms (McGraw-Hill, New York).

Sneddon, I. N. (1946). The distribution of stress in the neighborhood of a crack in an elastic solid. *Proceedings of the Royal Society of London. Series A,* 187, 229-260.

Sun, M., Lowry, G. V., & Gregory, K. B. (2013). Selective oxidation of bromide in wastewater brines from hydraulic fracturing. *Water Research,* 47, 3723-3731.

Vafi, K., & Brandt, A. (2016). GHGfrack: An Open-Source Model for Estimating Greenhouse Gas Emissions from Combustion of Fuel during Drilling and Hydraulic Fracturing. *Environmental Science & Technology*, *50*, 7913-7920.

Vengosh, A., Jackson, R. B., Warner, N., Darrah, T. H., & Kondash, A. A. (2014). Critical Review of the Risks to Water Resources from Unconventional Shale Gas Development and Hydraulic Fracturing in the United States. *Environmental Science & Technology,* 48, 8334-8348.

Weng, X. (1993). Fracture Initiation and Propagation From Deviated Wellbores. Society of Petroleum Engineers. doi:10.2118/26597-MS.

Xiong, B., Zydney, A. L., & Kumar, M. (2016). Fouling of microfiltration membranes by flowback and produced waters from the Marcellus shale gas play. *Water Research,* 99, 162-170

Yang, H., Liu, X., Yan, X., & Zhang, H. (2015). Discovery and reservoir-forming geological characteristics of the Shenmu Gas Field in the Ordos Basin. *Natural Gas Industry B,* 24, 295-306.